Ultrasonics Sonochemistry 84 (2022) 105959

Contents lists available at ScienceDirect

Ultrasonics Sonochemistry

journal homepage: www.elsevier.com/locate/ultson

Effect of ultrasonic power on the emulsion stability of rice bran protein-chlorogenic acid emulsion

Weining Wang [a], Ruiying Wang [b], Jing Yao [b], Shunian Luo [a], Xue Wang [a], Na Zhang [a], Liqi Wang [a,b,*], Xiuqing Zhu [a,*]

[a] College of Food Engineering, Key Laboratory of Food Science and Engineering of Heilongjiang Ordinary Higher Colleges/Key Laboratory of Grain Food and Comprehensive Processing of Heilongjiang Province, Harbin University of Commerce, Harbin 150028, China
[b] School of Computer and Information Engineering, Harbin University of Commerce, Harbin 150028, China

ARTICLE INFO

Keywords:
Ultrasound
Cavitation
Rice bran protein
Chlorogenic acid
Emulsion stability

ABSTRACT

In this study, rice bran protein–chlorogenic acid (RBP–CA) emulsion was subjected to an ultrasonic-assisted treatment technique. The encapsulation efficiency and loading capacity of chlorogenic acid (CA), and the morphology, particle size, zeta (ζ)-potential, atomic force microscopy image, viscosity, turbidity, and interfacial protein content of the emulsion under different ultrasonic power were investigated. The results revealed that the emulsion exhibited an encapsulation efficiency and loading capacity of 86.26 ± 0.11% and 17.25 ± 0.06 g/100 g, respectively, at an ultrasonic power of 400 W. In addition, the size of the emulsion droplets decreased and became more evenly distributed. Furthermore, the viscosity of the emulsion decreased significantly, and it exhibited a turbidity and interfacial protein content of 24,758 and9.34 mg/m^2, respectively. Next, the storage, oxidation, thermal, and salt ion stabilities of the emulsion were evaluated. The results revealed that the ultrasonic-assisted treatment considerably improved the stability of the emulsion.

1. Introduction

Emulsions are widely utilized in the production of several food products, such as ice cream, soybean milk, and beverages. In addition, it is one of the most promising drug delivery systems [1,2]. Ahmed et al. [3] prepared a curcumin nanoemulsion delivery system, which achieved a sustained release. The emulsion prevented the degradation of macromolecules in the gastrointestinal tract, ensures its successful passage through intestinal barriers, and facilitates drug absorption into the systemic circulation.

Emulsifiers that can mediate between phases are generally used to develop stable systems. However, the synthetic surfactants used during the preparation of emulsifiers are known to pose health risks, as it may cause intestinal dysfunction [4]. Over the past few decades, the number of consumers whom are aware of a healthier lifestyle is consistently increasing. Hence, the demand for natural, environmentally friendly, and healthy emulsifiers has increased.

Recently, plant-derived proteins have attracted widespread attention as emulsifiers. Particularly, Rice bran protein (RBP), which is obtained from agricultural by-products, has attracted significant attention owing to its high nutritional properties, low cost, and sustainability. Further, previous studies have demonstrated the easy digestibility and absorbability of RBP. In addition, RBP is used as a low-allergenic food for infants, the elderly, and individuals with allergies [5].

Studies have demonstrated that the combination of RBP and polyphenols improves the solubility and emulsification of RBP. Ju et al. fabricated a novel Pickering emulsion using protein isolate and anthocyanins, and found that the Pickering emulsion contained nutrients with health benefits [6]. Li et al. [7] demonstrated that the addition of (+)-catechin changed the 3D structure of protein and found that the emulsion of RBP and atechin complex exhibited a higher stability than the emulsion formed using natural RBP. Chlorogenic acid (CA), a natural phenolic acid [8], has attracted attention owing to its potential physiological functions, such as anti-oxidant capabilities [9], antibiotic action [10], and ability to reduce metabolic syndrome [11]. Wang et al. [12] reported that the addition of CA to RBP changed the structural and functional properties of RBP, and enhanced its solubility, emulsifying activity index, and emulsion stability index.

* Corresponding authors at: College of Food Engineering, Key Laboratory of Food Science and Engineering of Heilongjiang Ordinary Higher Colleges/Key Laboratory of Grain Food and Comprehensive Processing of Heilongjiang Province, Harbin University of Commerce, Harbin 150028, China.
E-mail address: hsdwlq@163.com (L. Wang).

https://doi.org/10.1016/j.ultsonch.2022.105959
Received 15 January 2022; Received in revised form 18 February 2022; Accepted 22 February 2022
Available online 1 March 2022

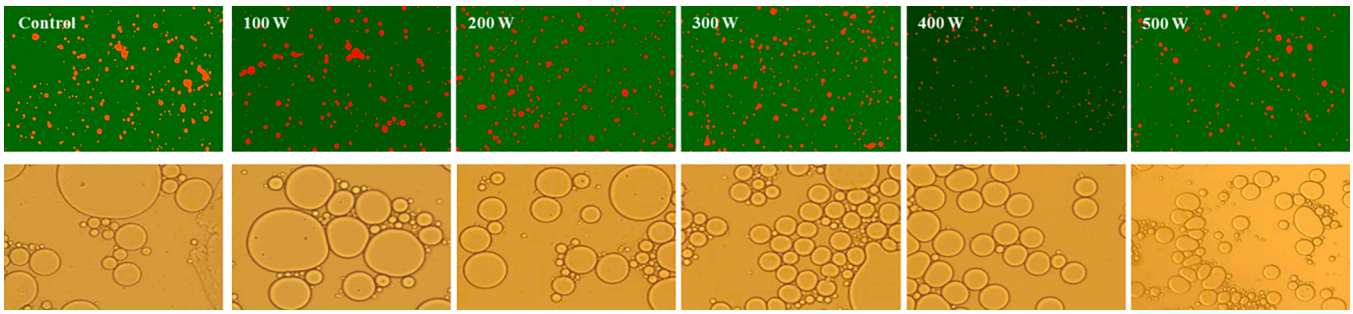

Fig. 1. Confocal laser microscope and optical microscope images of RBP-CA emulsion with different ultrasonic power.

Emulsion is a complex system, and its stability can be degraded by long-term storage, heating, and oxidation [13–15]. Nevertheless, its stability can be improved using high-energy physical methods, such as homogenization [16], microfluidizers treatment [17], and ultrasound/ultrasonic treatment [18]. Among these methods, ultrasound treatment has attracted attention as a safe, green, and efficient technology owing to its cavitation effect [19,20].

When ultrasonic waves pass through a medium, cavitation bubbles, which are rapidly formed and destroyed, affect temperature and pressure of the medium, thus inducing physical, chemical, and heat effects in the medium [21]. The application of ultrasonic technology during emulsification process induces physical effects, such as high pressure, shock waves, and micro jet [22,23]. Various studies have reported the effect of ultrasound treatment. Zhu et al. [24] prepared an evenly-distributed spherical composite (CL-20@PNA) emulsion using ultrasonic-assisted emulsification. In addition, Cucheval et al. [25] prepared an oil/water (O/W) emulsion using ultrasound-assisted emulsification, and found that the emulsion exhibited a uniform droplet distribution and a droplet size of approximately 0.7 μm at a treatment time of 5 min. Liu et al. [26] reported that high-intensity ultrasound treatment improved the physical stability of myofibrillar protein emulsion.

In this study, the encapsulation efficiency (EE) and loading capacity (LC) of CA, droplet morphology, particle size, ζ-potential, atomic force microscopy (AFM) image, apparent viscosity, and turbidity of the emulsion were determined, and the interfacial proteins were characterized. In addition, the stability of the emulsion was extensively investigated. This study aimed to investigate the effects of ultrasonic power on RBP–CA emulsion to enhance the application of RBP–CA emulsions.

2. Material and methods

2.1. Materials

Low-temperature defatted RBP was purchased from Great Northern Wilderness Agricultural Group Co., Ltd. (Harbin, China), and CA was purchased from TCI Chemical Industry Development Co., Ltd. (Shanghai, China). Soybean oil was purchased from Jiu San Group Harbin Grain and Oil Industry Group Co., Ltd (Harbin, China). All other chemicals (analytical grade) were purchased from Sinopharm Chemical Reagent Co., Ltd. (Shanghai, China).

2.2. Sample preparation

2.2.1. Extraction of RBP

Briefly, the low temperature defatted RBP was mixed with deionized water in a 1:15 ratio, and the pH value of the mixture was adjusted to 8.5 using 2 mol/L NaOH solution. Thereafter, the mixture was stirred at 200 rpm for 2 h, after which it was centrifuged for 15 min at 8000×*g*. Subsequently, the pH of the supernatant was adjusted to 4.5 using 2 mol/L HCl solution, after which the solution was centrifuged at 4500×g for 10 min to obtain a precipitate. The precipitate was washed twice using deionized water and adjusted to a pH of 7.0. The final sample was pre-frozen at −20 °C and freeze-dried.

2.2.2. Preparation of RBP–CA emulsion complex

Briefly, a protein solution (1%, w/v) containing 0.20% (w/v) CA was incubated for 2 h at 25 °C in the absence of oxygen. Subsequently, the liquid was placed in dialysis bag (cut off 10,000 Da, Bedford, MA, USA) at 4 °C for 48 h, and water was changed every 6 h. The dialysate was freeze-dried for use.

2.2.3. Preparation of O/W emulsions

In this study, O/W emulsions were prepared using the as-prepared RBP–CA complex emulsifier. The preparation flow chart is shown in Fig. 1. First, 70 mL of 2% RBP–CA emulsifier solution and 30 mL of soybean oil [27] were mixed using a high-speed homogenizer (T25 digital ULTRA-TURRAX, IKA, Germany). Subsequently, the mixture was subjected to ultrasonic treatment (Scientz Biotechnology Co., Ltd., Ningbo, China) for the ultrasonic-assisted emulsification at a power of 100, 200, 300, 400, and 500 W for 15 min. Lastly sodium azide (0.02% concentration) was added to the emulsion for subsequent analysis.

2.3. Characterization of RBP–CA emulsion

2.3.1. Determination of the EE and LC

The EE and LC of the emulsion were determined according the method described by Xu et al. [28]. EE was defined as the percentage of CA in complexes, and was evaluated using formula (1), and LC was defined as the percentage of CA that 1 g protein can load, and was evaluated using formula (2):

$$\mathrm{EE}(\%) = \mathrm{CA\ in\ emulsion/total\ CA} \times 100 \quad (1)$$

$$\mathrm{LC}(\%) = \mathrm{CA\ in\ emulsion/total\ protein} \times 100 \quad (2)$$

2.3.2. Confocal laser scanning microscopy (CLSM)

The distribution and size of the emulsion was examined using CLSM (Leica Microsystems, Heidelberg GmbH, Germany). To prepare the sample for this analysis, first, 1% isopropanol solution of Nile blue and 0.1% isopropanol solution of Nile red were prepared. Subsequently, 25 μL of the Nile blue solution and 20 μL of the Nile red solution were added to 0.5 mL of the prepared emulsions, after which the emulsion was mixed uniformly, filtered, and stood for 30 min. The determination process was based on the method of Jiang [29].

2.3.3. Orthographic microscopic imaging system analysis

For the orthographic microscopy imaging system analysis, 5 μL of the emulsion sample was placed in the center of a clean glass slide soaked in ethanol, and the sample was gently covered with a coverslip, and placed under a BX53 scientific research grade orthographic microscopic imaging system (Olympus China Co., LTD, Japan) to observe its microstructure at a magnification of 40×. Images were obtained in digital

processing software connected to a computer.

2.3.4. Particle size and ζ-potential determination

The particle size and ζ-potential of the emulsion were determined using Zetasizer Nano ZS (Malvern Instruments Ltd, Malvern, Worcestershire, U.K.) based on the method of Li et al. [30]. To measure the particle size, the emulsion was diluted to 0.2% (w/v), and filtered through a 0.45 μm pore size filter. To determine the ζ-potential,1 mL of the emulsion (concentration of 0.1 mg/mL) without any air bubbles was measured.

2.3.5. AFm

For the AFM analysis, the sample was scanned in a "tap" mode. Briefly, the emulsion (0.1% concentration) was placed on the surface of a mica sheet and dried in air. Subsequently, the AFM images were collected at room temperature at a driving and scanning frequency of 320 kHz and 1.0 Hz, respectively. The scanning area was 1 × 1 μm. The images and data were analyzed using Nano Scope Analysis 1.5 (Veeco, USA).

2.3.6. Apparent viscosity determination

To determine the apparent viscosity of the emulsion, the sample was placed on the sensor plate of rotary rheometer with a straight diameter, spacing, and shear rate of 40 mm, 15 mm, and 0.01–100 s^{-1}, respectively. For the analysis, 30 sampling points were selected at 25 °C at an equilibrium time of 1 min. Before the test, the sample to be tested was placed at room temperature for 30 min, after which 2 mL of the emulsion was placed on the gap of the plate, and the sample was covered with silicone oil.

2.3.7. Emulsion turbidity determination

The turbidity of the emulsion was determined based on the method of Li et al. [31] with appropriate modifications. Briefly, the emulsion was diluted 40 times using 10 mmol/L phosphate buffer solution (pH 7.0), and phosphate buffer solution was used as a blank control. The absorbance of the emulsion at 600 nm was measured using an ultraviolet–visible (UV–Vis) spectrophotometer (UNICO UV-2100, Shanghai, China). The turbidity was calculated using formula (3):

$$T = 2.302\,AV/I \tag{3}$$

Where A is the absorbance of the diluted emulsion at 600 nm, V is the dilution factor, and I is the optical path difference of 0.01 m.

2.3.8. Interfacial protein content determination

The separation of the interface-adsorbed proteins was examined based on the method of Yi et al. [31] with appropriate modifications. Briefly, the fresh emulsion was centrifuged for 60 min (18000×*g*, 4 °C), after which the emulsifying layer was separated. Subsequently, phosphoric acid buffer solution (10 mmol/L, pH 7) was added to the separated emulsifying layer, after which the solution was centrifuged for 30 min (18000 × g, 4 °C). The emulsion layer was evenly mixed with acetone in a ratio of 1:20, and centrifuged for 40 min (18000 × g, 4 °C), after which the supernatant was stood for 2 h at 18 °C. The precipitate was washed five times using acetone and two times using water. Subsequently, the precipitate was freeze-dried, after which the interfacial-adsorbed proteins were obtained. The interface-adsorbed protein content was evaluated using formula (4):

$$\Gamma = \frac{V_C(C_{INI} - C_{SER})}{SV_{OIL}} = \frac{(1-\phi)d_{32}}{6\phi}(C_{INI} - C_{SER}) \tag{4}$$

where Γ is the Interfacial protein content, V_C is the volume of the water phase, V_{OIL} is the volume of the oil phase, ∅ is the volume fraction of the oil phase, C_{INI} is the initial RBP-CA concentration, C_{SER} is the residual RBP-CA concentration of water phase after emulsification.

Table 1
EE and LA of CA in RBP-CA emulsion with different ultrasonic power.

	Control	100 W	200 W	300 W	400 W	500 W
EE (%)	81.77 ± 0.15^{f}	84.41 ± 0.26^{e}	85.13 ± 0.08^{d}	85.86 ± 0.28^{c}	86.26 ± 0.11^{a}	86.04 ± 0.07^{b}
LC (g/100 g protein)	16.34 ± 0.04^{f}	16.88 ± 0.02^{e}	16.94 ± 0.07^{d}	17.17 ± 0.04^{c}	17.25 ± 0.06^{a}	17.21 ± 0.05^{ab}

2.4. Determination of the emulsion stability

2.4.1. Chromatographic index (CI) determination

Briefly, the fresh emulsion was placed in a 10 mL clear glass bottle, and the samples were sealed and stored at room temperature, away from light. The upper layer was an emulsion layer and the lower layer was a clear layer. The CI was calculated using formula (4).

$$CI = \frac{H_c}{H_t} \tag{5}$$

where H_c is the height of the clear liquid layer at the bottom and H_t is the height of total emulsion.

2.4.2. Oxidative stability determination

To determine the oxidative stability, the emulsions were oxidized at 60 °C, and the peroxide value (PV) and the content of secondary oxidation product (TBARS) were determined. Briefly, 0.3 mL of the emulsion, 1 mL of isooctane, and 0.5 mL of isopropyl alcohol were placed in a centrifugal tube, mixed, and centrifuged at 2000 × g for 10 min. Thereafter, 0.6 mL of the liquid supernatant, 4.6 mL of methanol, and 2.8 mL of butanol were mixed together. In addition, 45 μL of 3.9 mol/L potassium thiocyanate and 45 μL of 0.072 mol/L Fe^{2+} were thoroughly mixed, and reacted in the dark at room temperature for 20 min. Subsequently, the absorbance was measured at 510 nm using a UV spectrophotometer. A methanol/butanol mixture was used as the blank sample, and 30% hydrogen peroxide was used as standard material to draw the standard curve. The determination of TBARS was based on the method of Ym A [32].

2.4.3. Thermal stability determination

The thermal stability of the emulsion was evaluated by examining the change in the particle size, Polydispersity index (PDI), andζ-potentials of the sample at 70 °C for 0.5 h (pasteurization).

2.4.4. Saline ion stability determination

The determination of the saline ion stability was based on the method of Dongze Li [33] with slight modifications. The saline ion stability was evaluated by examining the change in the particle size, PDI, and potential of emulsion at different saline ion concentration (0, 200, and 400 mM) for 0.5 h.

2.5. Statistical analysis

The data obtained in this research were calculated by averaging the results of three parallel experiments. The software used in this study included Origin 8.5, SPSS 22.0, Nano Scope Analysis 1.5 and Peakfit V4.12. The significant difference was analyzed using one-way analysis of variance (ANOVA) and Duncan's test ($p < 0.05$).

3. Results and discussion

3.1. Characterization of the RBP–CA emulsion

3.1.1. EE and LC analysis

The EE and LC of all the emulsion samples were higher than 80% and 16 g/100 g protein, respectively (Table 1), which is consistent with the

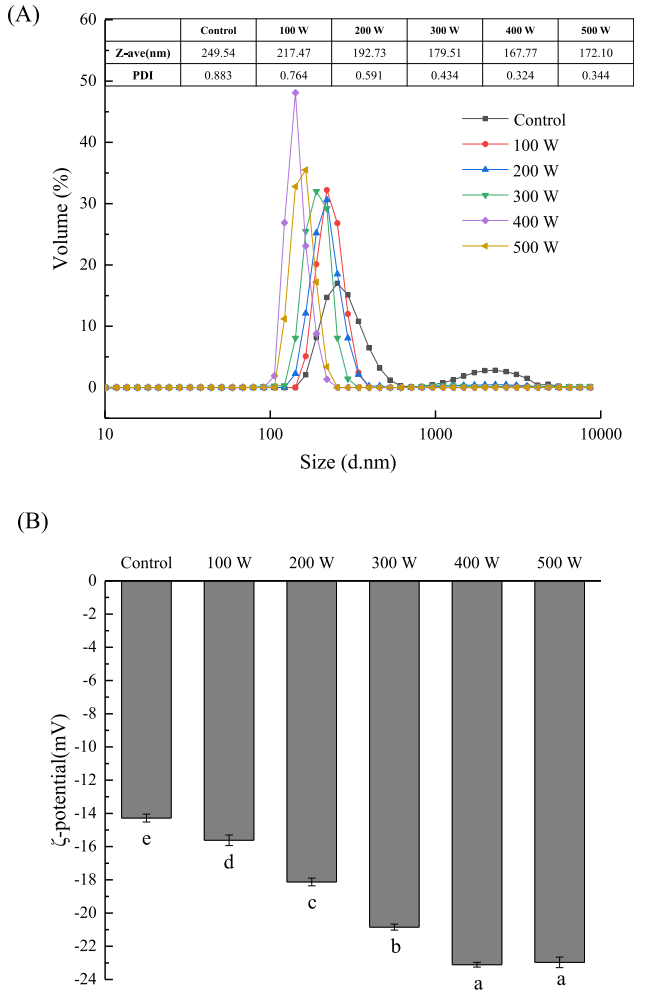

Fig. 2. Particle size (A) and ζ-potential (B) of RBP-CA emulsion with different ultrasonic power.

findings of Xu et al. [28]. After the ultrasonic-assisted treatment, the EE and LC of polyphenol (i.e., CA) in the RBP separation emulsion increased to 83.85 ± 0.43% and 15.68 ± 0.070 g/100 g protein, respectively. This higher EE and LC could be majorly attributed to the fact that ultrasonic waves affected the temperature and pressure in the emulsion system and induced physical, chemical, and heat effects on the emulsion. With an increase in the ultrasonic power, the EE and LC of the system increased significantly. At an ultrasonic power of 400 W, the EE and LC values were 86.26 ± 0.11% and 17.25 ± 0.06 g/100 g protein, respectively, which were the highest values observed in this study. This may be attributed to the destruction of the protein spatial structure and promotion of the unfolding of the RBP by the ultrasonic cavitation. In addition, the number of sites where proteins could bind with CA increased. Furthermore, the micro-jet action induced by the ultrasonic-assisted treatment enhanced the dispersion of the emulsion droplets. Consequently, the stability of the emulsion system increased, thus increasing its EE and LC. However, a further increase in the intensity of the ultrasonic-assisted treatment resulted in the re-aggregation of the unfolded protein structure, thus decreasing the EE and LC of the RBP–CA emulsion.

3.1.2. Emulsion morphology analysis

To investigate the morphology of the drops, the sample was stained and observed using CLSM and scientific research grade orthographic microscopic imaging system. The oil droplets were observed to be covered with protein (Fig. 2) [29]. Furthermore, the droplets exhibited a spherical shape, indicating that the emulsion was an O/W emulsion. In addition, there were some differences in the particle size and distribution state of the emulsions. The emulsion prepared without ultrasound-assisted treatment exhibited an unevenly distributed microstructure and a large average droplet diameter. In contrast, the ultrasonic-treated RBP emulsions droplets exhibited a more even dispersion and decreased particle size. In addition, the emulsion exhibited significantly enhanced stability, and the spherical droplets remained well separated without significant flocculation. With an increase in the ultrasonic power, the droplets increased in size and became more uniformly distributed. This could be attributed to the fact that the cavitation effect of the ultrasonic treatment resulted in a decrease in the particle size of the emulsion, thus inducing a rapid and even distribution of the RBP–CA emulsifier at the O/W interface. Consequently, a thick protein film that could withstand oil drop was formed and exhibited a higher oil droplet coating rate. With a further increase in the ultrasonic power to 500 W, the morphology of the emulsion droplet changed significantly. The re-aggregation of the uniformly dispersed droplets may be attributed to the thermal effect of the ultrasound treatment. Wu et al. [34] revealed that ultrasonic assistance had a positive impact on the particle size and distribution of emulsions, which is consistent with the findings of this study.

3.1.3. Particle size and ζ-potential analysis

Particle size has an important effect on the stability and other functional properties of protein emulsions. The PDI reflects the uniformity of the particle size distribution of emulsions. Studies have demonstrated that a smaller particle size and more uniform distribution could improve the stability of emulsion [35]. The particle size of the emulsion changed with an increase in the ultrasonic power (Fig. 3A). Without ultrasonic treatment, the emulsion exhibited a bimodal particle distribution and a relatively large particle size. However, the particle size and PDI of RBP decreased after the ultrasonic assisted treatment, which corresponded to a good application prospect. After homogenization, a coarse emulsion was formed; however, the emulsion was not sufficiently stable owing to the large particle size of the droplet, and the emulsifier was not evenly distributed at the O/W interface. After the ultrasound-assisted treatment, cavitation bubbles were generated under the strong cavitation physical action. Owing to the strong kinetic energy of the bubbles, the bubbles broke down the large particle-sized droplets, thus resulting in a more uniform and stable emulsion system. With an increase in the ultrasonic power, the cavitation yield increased, the number of generated bubbles increased, and the bubble size decreased, thus increasing the emulsion stability. However, with a further increase in the ultrasonic power to 500 W, the particle size and PDI of the emulsion exhibited an increasing trend. This phenomenon may be explained as follow: As the cavitation effect became significantly strong, the smaller droplets were forcefully squeezed and re-aggregated together. In addition, this could be attributed to the destruction of droplets by the thermal effect of the ultrasound treatment. The accumulation of damaged droplets resulted in the formation of uneven aggregates, which resulted in a larger particle size. Jna et al. [36] evaluated the potential application of ultrasonic treatment for the preparation of (GPP) nanoemulsion in mustard oil, and found that the droplet size decreased significantly after the ultrasonic treatment, and the particles were largely spaced, which is consistent with the morphology observation in this study.

Generally, the ζ-potential is used to indicate the strength of electrostatic interaction. The electrostatic repulsion between droplets increases with an increase in the absolute potential value. Therefore, it is a key indicator of emulsion stability. The ζ-potential of the RBP–CA emulsion samples under different ultrasonic treatment conditions are shown in Fig. 3(B), and the results reveal that the potentials of all the samples were negative. In addition, the untreated emulsions exhibited the lowest absolute ζ potential value. The absolute ζ- potential values of the treated RBP–CA emulsions significantly increased with an increase in the ultrasonic power. At anultrasonic power of 400 W, the absoluteζ-

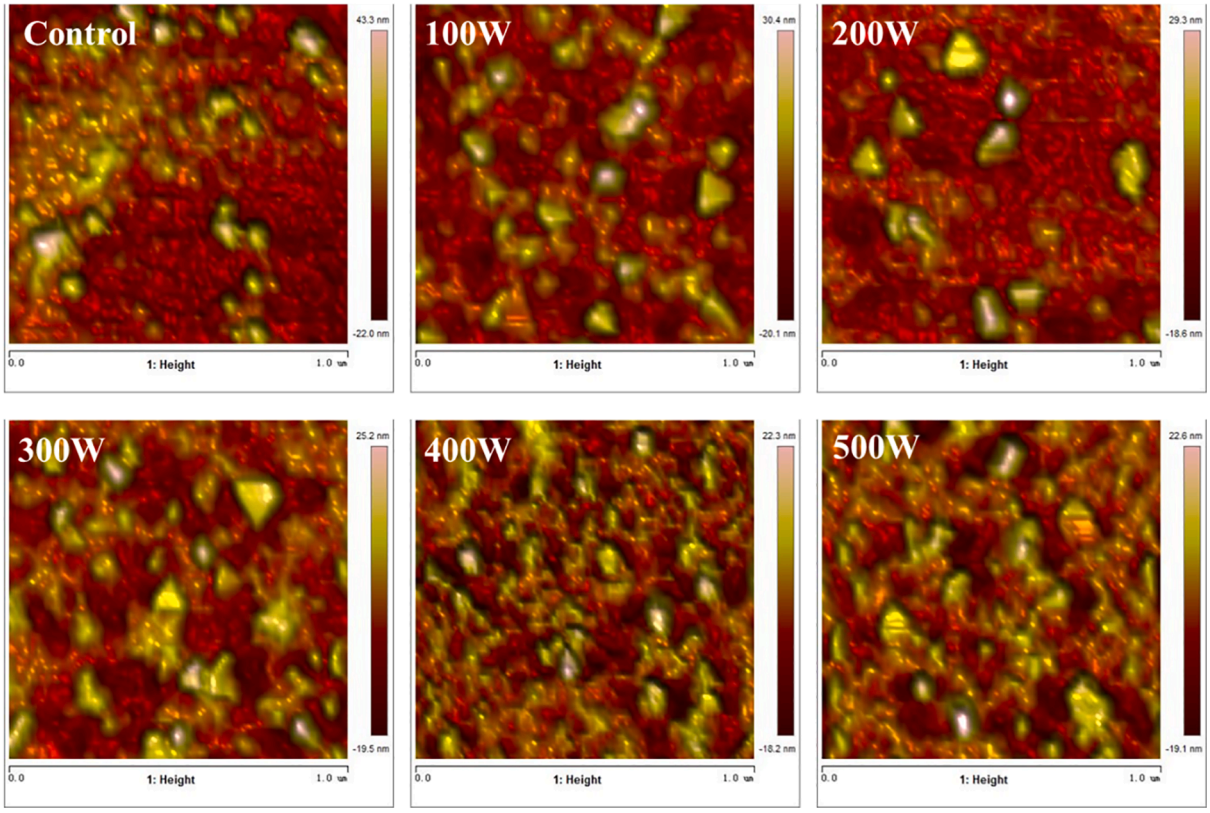

Fig. 3. AFM images of RBP-CA emulsion with different ultrasonic power.

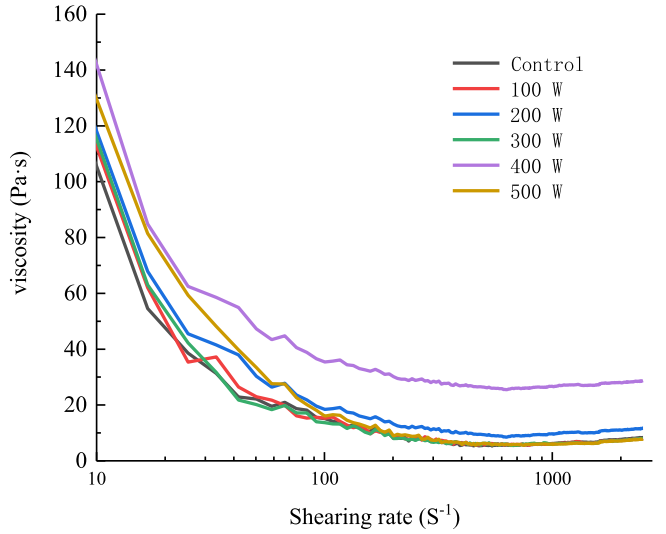

Fig. 4. Apparent viscosity of RBP-CA emulsion with different ultrasonic power.

potential value increased to 23.11 mV. This could be attributed to the opening up of the initially dense protein structures by the ultrasonic-assisted treatment, which resulted in the exposure of the initially-embedded polar groups to the surface of each protein particle. The increase in the charge of the exposed groups resulted in an increase in the absolute ζ-potential value. In addition, the ultrasonic treatment affected the charge distribution on the surface of the emulsion droplet. The increase in the ζ-potential increased the electrostatic repulsion between the emulsion droplets and inhibited aggregation, thus improving the stability of the complex emulsion. However, a further increase in the ultrasonic power resulted in protein aggregation to some extent. Consequently, the polar potential of drops surface was covered and the absolute ζ-potential value decreased at 500 W.

3.1.4. AFM analysis

The microstructure of the RBP–CA emulsion deposited on mica sheet was observed using AFM, and the 3D structure of the samples was analyzed using Nanoscope Analysis software, and the result is shown in Fig. 4. Without ultrasonic treatment, the RPB–CA emulsion exhibited a disordered aggregation state. In contrast, the emulsion exhibited a significantly enhanced uniform droplet distribution after the ultrasonic treatment. When the ultrasonic power was<400 W, the particle size of the emulsion decreased with an increase in the ultrasonic power. In addition, the number of droplets per unit area was higher than in the untreated emulsions. With a further increase in the ultrasonic power to

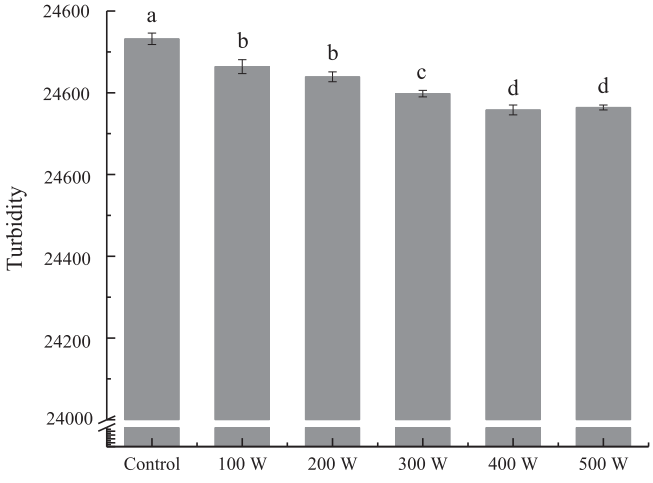

Fig. 5. Turbidity of RBP-CA emulsion with different ultrasonic power.

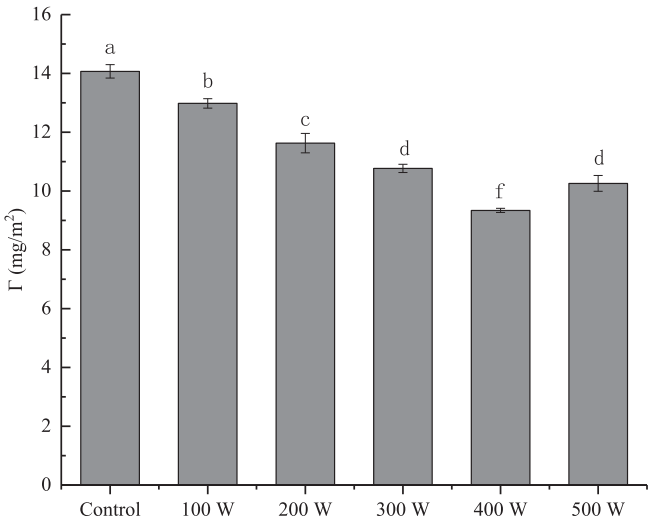

Fig. 6. Interfacial adsorption protein content of RBP-CA emulsion with different ultrasonic power.

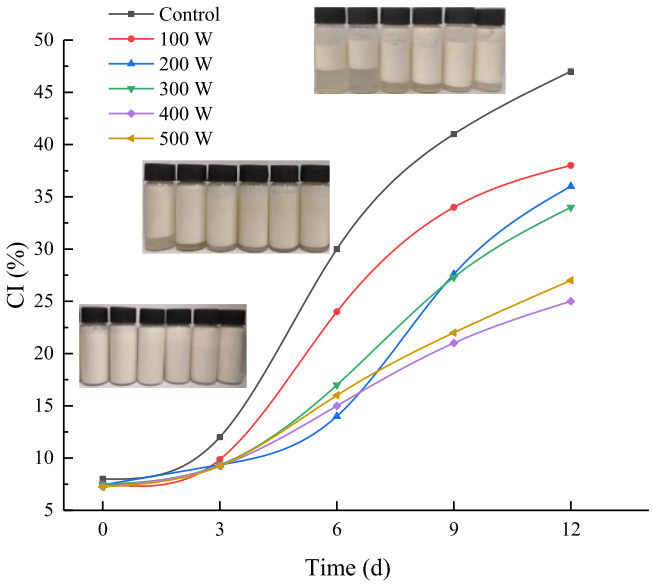

Fig. 7. CI of RBP-CA emulsion with different ultrasonic power.

500 W, the particle size and PDI increased. The thickness of the interface film was characterized using the average height in tap mode. Compared to the untreated emulsion, the interface film thickness of the treated emulsion increased to 21.03 nm. Roughness average (Ra) value, as a basic statistical parameter, could reflect the roughness of a sample surface and the aggregation degree. The Ra value of the treated samples was 1.98 nm, which was significantly lower than that of the untreated samples (Ra = 13.91 nm). The decreased Ra indicated that ultrasonic treatment can change the distribution of RBP–CA particles within a certain range. The high energy physical action of the ultrasonic-assisted treatment facilitated the formation of the interface film and its uniform dispersion. At an ultrasonic power of 500 W, the dispersed droplets re-aggregated, thus increasing the Ra value.

3.1.5. Apparent viscosity analysis

According to Stoke's law, the upward floating rate of droplets decreases with an increase in the viscosity of an emulsion system, which enhances the stability of the emulsion [37]. The apparent viscosity of the ultrasound-treated emulsions decreased with an increase in the shear rate, resulting in the shear thinning of non-Newtonian fluids (Fig. 5). In the absence of shear force, fluid molecules intertwined with each other. Under the action of shear force, the fluid force destroyed the flocculants in the system, and broke down the accumulated fat globules. In addition, the droplet directional arrangement resistance and the emulsion apparent viscosity decreased. When the shear rate was increased to a certain value, the intermolecular alignment was complete and the viscosity did not change [38]. The apparent viscosity of the emulsion first increased and then decreased with an increase in the ultrasonic power, and the emulsion apparent viscosity reached a peak with an increase in the ultrasonic power to 400 W. With an increase in the ultrasonic power, the particle size of the emulsion decreased, and the number of droplets in the dispersed phase increased. In addition, the potential for two droplets to enter the mutual attraction region increased rapidly, which negatively affected the displacement and resulted in an increase in the apparent viscosity of the emulsion. With a further increase in the ultrasonic power to 500 W, the apparent viscosity of the emulsion decreased.

3.1.6. Emulsion turbidity analysis

As a macro index, turbidity can measure the turbidity degree of emulsion, which is not only related to droplet size, but also closely related to the droplet shape and distribution. The turbidity of the emulsion negatively correlated with its stability. Fig. 6 shows the turbidity of the ultrasonic-treated emulsion at different ultrasonic powers. After ultrasonic treatment, the turbidity of the emulsion changed significantly. With an increase in the ultrasonic power, the turbidity first decreased and then increased. At an ultrasonic power of 400 W, the lowest turbidity (24758) of the emulsion was observed. With a further increase in the ultrasonic power to 500 W, the turbidity of the emulsion increased. This trend is consistent with the particle size results. This could be attributed to the fact that the strong physical force of the ultrasonic waves after the ultrasonic treatment crushed the droplets, which resulted in a decreased particle size, more uniform droplet distribution, and decreased turbidity. However, with a further increase in the ultrasonic power to 500 W, the thermal effect of the ultrasonic treatment resulted in the aggregation of droplets, thus resulting in an increase in the emulsion turbidity.

3.1.7. Analysis of the interfacial protein content

The content of the adsorbed protein at the RBP–CA emulsion interface with a change in the ultrasonic power is shown in Fig. 7. Without ultrasonic treatment, the content of the interface-adsorbed protein of the RBP emulsion was 14.07 mg/m^2, which decreased to 9.34 mg/m^2 after 400 W ultrasonic treatment. However, the content of interfacial adsorption protein increased significantly with a further increase in the ultrasonic power. Generally, the ultrasonic treatment reduces the content of interfacial adsorbed protein, which might be attributed to the unfolding of the structure of the interface-adsorbed protein by the cavitation effect. However, a further increase in the ultrasonic power increased the content of the interface-adsorbed protein by inducing the formation of aggregates by the interface-adsorbed protein. Furthermore, excessive treatment conditions resulted in a decrease in the emulsion stability, which may be attributed to the fact that the interface-adsorbed protein with excessively high content can be squeezed by Coulomb force, which can promote the formation of a rigid interface film by the interface-adsorbed protein. Similarly, the enhanced emulsions stability under moderate ultrasonic power could be attributed to the formation of more flexible and viscoelastic interface membranes by the interface-adsorbed proteins with a higher content [39].

3.2. Analysis of the emulsion stability

3.2.1. CI analysis

The CI of emulsions refers to the degree of aggregation and separation of the oil phase and water phase during storage, and it can be used

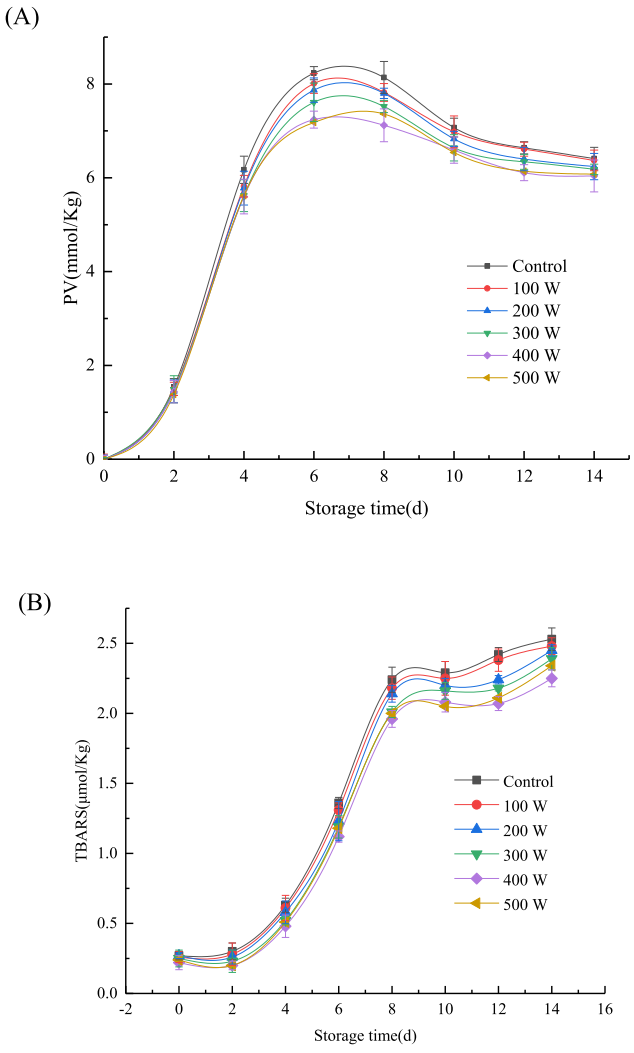

Fig. 8. Oxidation stability of RBP-CA emulsion with different ultrasonic power.

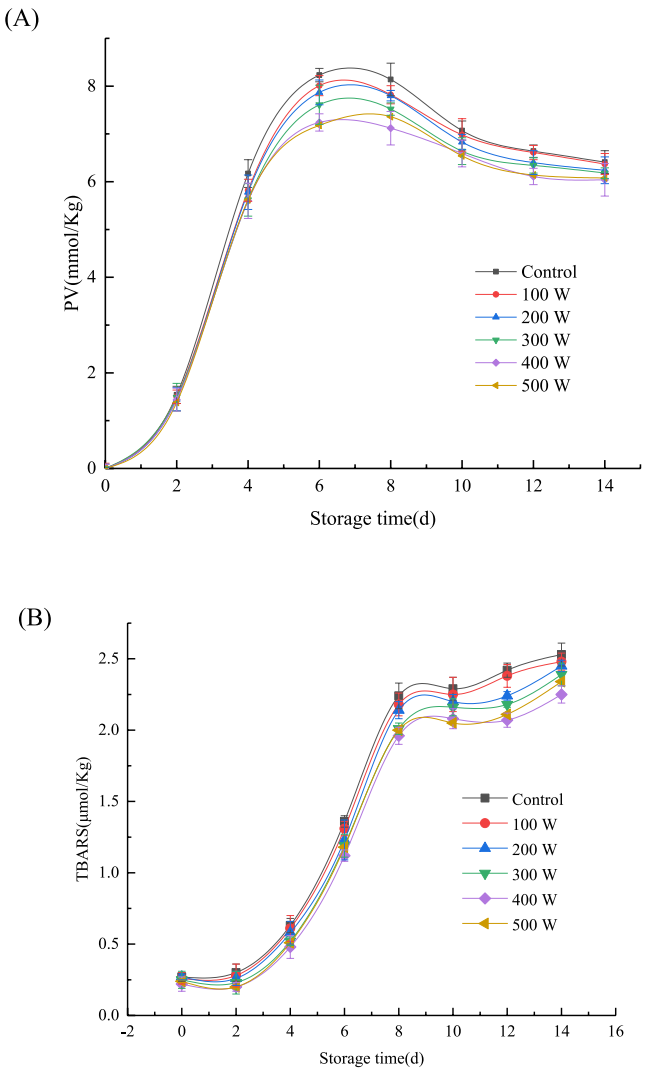

Fig. 9. Oxidation stability of RBP-CA emulsion with different ultrasonic power. (A) reflects the change of PV value with storage time. (B) reflects the changes of TBARS values with storage time.

to evaluate the storage stability of emulsions. Fig. 8 shows the change in the CI of the emulsion samples under different ultrasonic treatment conditions. The freshly prepared RBP–CA emulsion exhibited a uniform milky white color. With an increase in the storage time, all samples exhibited a notable stratification phenomenon, but none of the samples exhibited the oil floating phenomenon during storage. These result indicated that the emulsions exhibited a good storage stability. The untreated emulsion exhibited the highest CI during the storage process. The ultrasonic-assisted reduced the CI of the emulsions and effectively prevented the separation of the oil phase and water phase. In addition, the repulsive force between the treated oil droplets coated with more RBP–CA increased. This is because it effectively inhibited the coalescence and phase separation of the emulsions. The complex emulsions exhibited the best storage stability at an ultrasonic power of 400 W. This indicated that the ultrasonic-assisted treatment can change the structure of RBP–CA, which enhanced the close bonding between RBP-CA and oil droplets, thus improving the stability of emulsion. Omid [40] revealed that the stability of O/W emulsion significantly improved after ultrasonic treatment, which is consistent with the findings of this study After storage for six days, there was no significant difference in the storage stability of the emulsions at all the ultrasonic intensities (200, 300, 400, and 500 W); however, a significant difference was observed after storage for nine days, which could be attributed to the significantly small emulsion surface potential change, and the deposition and aggregation of the emulsion on the ninth day [41].

3.2.2. *Oxidative stability analysis*

Hydro peroxides and malondialdehyde are produced by the lipid oxidation of emulsions during storage. The primary oxidation degree of oil can be reflected by the PV value, and the secondary oxidation degree of oils can be characterized using the TBARS values [42]. The oxidation stability results of the emulsion are shown in Fig. 9, where (A) represents the first-grade oxidation degree of the oil and (B) represents the second-grade oxidation degree of the oil. The PV values of all samples increased rapidly during the first seven days of storage, after which it decreased gradually. In contrast, TBARS values increased rapidly after seven days. This could be mainly attributed to the degradation of the primary oxidation products of oil, which resulted in the accumulation of the secondary oxidation products. Particularly, this was manifested in the increase of the TBARS value of the malondialdehyde content. The lowest PV and TBARS values were observed at an ultrasonic power of 400 W owing to the higher oxidation stability of the emulsion at this power. Studies have revealed that protein containing a large amount of phenolic hydroxyl, acid, basic amino acid and hydrophobic amino acid tyrosine exhibit antioxidant activity [43]. In addition, the aromatic ring-contained hydroxyl groups, and the hydrogen in this ring could scour free radicals and terminate the free radical chain. The mechanism involved in the resistance of oxidation by acidic and basic amino acids can be attributed to their binding to metal ions. Hydrophobic amino

Table 2
Thermal stability of RBP-CA emulsion with different ultrasonic power.

	Heat	Control	100 W	200 W	300 W	400 W	500 W
Z-Ave (d.nm)	Before	249.54 ± 2.41^{a}	217.47 ± 3.65^{b}	192.73 ± 2.62^{c}	179.51 ± 1.91^{d}	167.77 ± 2.47^{f}	172.10 ± 3.96^{e}
	After	907.95 ± 31.72$^{a'}$	804.73 ± 3.51$^{b'}$	616.3 ± 2.49$^{c'}$	494.96 ± 2.57$^{d'}$	388.57 ± 2.61$^{f'}$	424.63 ± 2.14$^{e'}$
PDI	Before	0.883 ± 0.085^{a}	0.764 ± 0.061^{ab}	0.591 ± 0.093^{c}	0.440 ± 0.077 ^{cd}	0.318 ± 0.034^{def}	0.344 ± 0.103^{de}
	After	0.904 ± 0.052$^{a'}$	0.799 ± 0.027$^{b'}$	0.646 ± 0.084$^{c'}$	0.511 ± 0.038$^{d'}$	0.349 ± 0.052$^{d'f'}$	0.409 ± 0.087$^{d'e'}$
ζ-potential (mV)	Before	−14.28 ± 0.34^{f}	−15.63 ± 0.67^{e}	−18.13 ± 0.76^{d}	−20.85 ± 0.35^{c}	−23.11 ± 0.71^{a}–	−22.97 ± 0.43^{ab}
	After	−13.89 ± 0.84$^{d'e'}$	−14.23 ± 0.71$^{d'}$	−17.59 ± 0.50$^{c'}$	−18.94 ± 0.63$^{b'}$	−21.76 ± 0.31$^{a'}$	−21.34 ± 0.51$^{a'b'}$

Note: The values with different superscript letters within a column are significantly different ($p < 0.05$).

Table 3
Saline ions stability of RBP emulsion with different ultrasonic power.

	Salt ion concentration	Control	100 W	200 W	300 W	400 W	500 W
Z-Ave(d.nm)	0	249.54 ± 2.41^{a}	217.47 ± 3.65^{b}	192.73 ± 2.62^{c}	179.51 ± 1.91^{d}	167.77 ± 2.47^{f}	172.10 ± 3.96^{e}
	200	333.57 ± 2.87$^{a'}$	276.26 ± 4.37$^{b'}$	214.37 ± 3.64$^{c'}$	176.51 ± 5.24$^{d'}$	152.37 ± 3.76$^{e'f'}$	153.67 ± 4.53$^{e'}$
	400	461.34 ± 3.76$^{a''}$	398.71 ± 6.34$^{b''}$	328.51 ± 2.58$^{c''}$	281.63 ± 5.30$^{d''}$	238.67 ± 4.84$^{f''}$	264.26 ± 2.89$^{e''}$
PDI	0	0.883 ± 0.085^{a}	0.764 ± 0.064^{ab}	0.591 ± 0.093^{c}	0.440 ± 0.077 ^{cd}	0.318 ± 0.034^{ef}	0.344 ± 0.103^{de}
	200	N.D.	0.937 ± 0.022$^{a'}$	0.735 ± 0.063$^{b'}$	0.673 ± 0.051$^{c'}$	0.494 ± 0.083$^{d'e'}$	0.503 ± 0.084$^{d'}$
	400	N.D.	N.D.	0.961 ± 0.038$^{''}$	0.846 ± 0.014$^{b''}$	0.703 ± 0.046 $^{cd''}$	0.736 ± 0.061$^{c''}$
ζ- potential (mV)	0	−14.28 ± 0.34^{f}	−15.63 ± 0.84^{e}	−18.13 ± 0.76^{d}	−20.85 ± 0.35^{c}	−23.11 ± 0.71^{a}	−22.97 ± 0.43^{ab}
	200	−4.57 ± 0.53$^{f'}$	−6.82 ± 0.53$^{a'b'c'd'e'}$	−7.31 ± 0.63$^{a'b'c'd'}$	−7.47 ± 0.31$^{a'b'c'}$	−7.69 ± 0.69$^{a'}$	−7.62 ± 0.84$^{a'b'}$
	400	−1.94 ± 0.27$^{d''e''f''}$	−2.23 ± 0.13$^{b''c''d''e''}$	−2.44 ± 0.28$^{a''b''c''d''}$	−2.58 ± 0.44$^{a''b''c''}$	−2.84 ± 0.32$^{a''}$	−2.73 ± 0.51$^{a''b''}$

Note: The values with different superscript letters within a column are significantly different ($p < 0.05$).

acids could increase the presence of polypeptides at the O/W interface and improve the scavenging activity of hydrophobic or lipid phase free radicals [44]. The addition of CA enhanced the antioxidant capacity of the emulsion. In addition, the ultrasonic-assisted treatment changed the structure of the protein, this enhancing their ability to bind with CA, which enhanced the exposure of more groups conducive to the antioxidant. In the RBP–CA emulsion system, the oil phase was more firmly encapsulated. At an ultrasonic power of 500 W, the emulsions were oxidized by heat. Several studies have reported the application of ultrasonic technology for the antioxidation of emulsions. For example, Niu et al. [45] enhanced the retention of β-carotene activity by wrapping β-carotene in an emulsion. JNA et al. [36] extended the oxidation stability of mustard oil using ultrasonic-treated emulsion

3.2.3. Thermal stability analysis

Heat treatment is one of the most commonly used techniques in food processing, as it can kill microorganisms in food and improve safety. Therefore, emulsions should exhibit a good thermal stability. The thermal stability of the emulsions was evaluated by investigating the change in particle size, PDI, and ζ-potential. The change in the ultrasonic power had no significant effect on the PDI of the emulsions, but significantly changed the average particle size and ζ-potential of the emulsion (Table 2). The untreated emulsion exhibited the highest average particle size. The stability of the emulsion was destroyed by heating, and the droplets coalesced and the particle size became uneven. Compared to the untreated emulsion, the average particle size of the ultrasonic-treated emulsions decreased significantly after heating. Particularly, after heating, the average particle size of the emulsion at an ultrasonic power of 400 W was 388.57 ± 2.61 nm. In addition, the ultrasonic treatment reduced the stratification of the emulsions owing to the enhanced even distribution of the emulsion droplets after the ultrasonic-assisted treatment. Particularly, the ultrasonic-assisted treatment enhanced the stability of the emulsion system and its resistance of heat. However, with a further increase in the ultrasonic power beyond 400 W, the average particle size increased, indicating that the physical and chemical effects caused by the ultrasonic treatment resulted in the disorder of the internal structure of the emulsion, which negatively affected the thermal stability of the emulsion.

3.2.4. Saline ion stability analysis

Typically, saline ions are mixed with emulsions. Therefore, it is essential to investigate the saline ion stability of emulsions. The influence of saline ions on the stability of the emulsion is shown in Table.3. Compared to the emulsion without saline ions, the particle size of the emulsion containing saline ions changed significantly. At a salt ion concentration of 200 mM, an aggregation of the emulsion was observed, and the sizes of the droplets were larger than 150 nm. At a salt ion concentration of 400 mM, the particle size of the emulsion changed significantly, indicating the damage of the stability of the emulsion system. The ultrasonic-assisted treatment improved the salt ion stability of the emulsion. The addition of saline ions to the emulsion resulted in a change in the surface charge of the emulsion. Therefore, polymerization occurred owing to the interaction between the hydrophobicity of the emulsion and the net charge of the emulsion droplet. The absolute ζ-potential value decreased significantly at a saline ion concentration of 400 mM. This weakened the electrostatic force between the emulsions, and resulted in the aggregation of the emulsion. After the ultrasonic-assisted emulsification, the particle size of the emulsion decreased after the addition of salt ions, and the salt ion resistance of the emulsion increased. Emulsions with a high salt tolerance exhibit a high potential for industrial application, indicating the promising application potential of the ultrasonic-treated emulsions prepared in this study. This findings of this analysis are consistent with the findings of MA et al. [46] who reported that ultrasound-treated protein peptide emulsions exhibited enhanced ionic, thermal, and storage stability, and reduced lipid oxidation.

4. Conclusion

In this study, RBP–CA emulsion was prepared using ultrasonic-assisted treatment, and the effect of ultrasonic power on the emulsion stability of the RBP–CA emulsion was investigated. The results revealed that the ultrasonic-assisted treatment improved the EE and LC of the emulsion, decreased the particle size of the emulsion, enhanced the uniform distribution of the droplets, and enhanced the viscosity of the emulsion. In addition, the ultrasonic-assisted treatment reduced the aggregation of droplets and interfacial protein, and the flocculation and stratification of the emulsion during storage. Furthermore, it enhanced the oxidation resistance, heat resistance, and salt ion interference resistance of the emulsion. The finding of this study is expected to enhance the application of ultrasound treatment for the preparation of stable emulsions.

CRediT authorship contribution statement

Weining Wang: Conceptualization, Methodology, Software, Investigation, Formal analysis, Writing – original draft. **Ruiying Wang:** Data curation, Writing – original draft. **Jing Yao:** Visualization, Investigation. **Shunian Luo:** Resources, Supervision. **Xue Wang:** Software, Validation. **Na Zhang:** Visualization, Writing – review & editing. **Liqi Wang:** Conceptualization, Funding acquisition, Resources, Supervision, Writing – review & editing. **Xiuqing Zhu:** Conceptualization, Funding acquisition, Resources, Supervision, Writing – review & editing.

Declaration of Competing Interest

The authors declare that they have no known competing financial interests or personal relationships that could have appeared to influence the work reported in this paper.

Acknowledgements

This work was supported by a grant from “Major science and technology Program of Heilongjiang (Program No.2020ZX08B02).

References

[1] W. Lu, A.L. Kelly, S. Miao, Emulsion-based encapsulation and delivery systems for polyphenols, Trends Food Sci. Technol. 47 (2016) 1–9.
[2] C. Güell, M. Ferrando, A. Trentin, K. Schron, Apparent interfacial tension effects in protein stabilized emulsions prepared with microstructured systems, Membranes 7 (2) (2017) 19.
[3] K. Ahmed, L. Yan, D.J. Mcclements, X. Hang, Nanoemulsion- and emulsion-based delivery systems for curcumin: encapsulation and release properties, Food Chem. 132 (2) (2012) 799–807.
[4] L. Tmáková, S. Sekretár, Š. Schmidt, Štefan Schmidt, Plant-derived surfactants as an alternative to synthetic surfactants: surface and antioxidant activities, Chem. Pap. 70 (2) (2016), https://doi.org/10.1515/chempap-2015-0200.
[5] R. Satoh, I. Tsuge, R. Tokuda, R. Teshima, Analysis of the distribution of rice allergens in brown rice grains and of the allergenicity of products containing rice bran, Food Chem. 276 (2019) 761–767.
[6] M. Ju, G. Zhu, G. Huang, X. Shen, X. Sui, A novel pickering emulsion produced using soy protein-anthocyanin complex nanoparticles, Food Hydrocolloid 99 (2019), 105329.
[7] D. Li, Y. Zhao, X. Wang, H. Tang, N. Wu, F. Wu, D. Yu, W. Elfalleh, Effects of (+)-catechin on a rice bran protein oil-in-water emulsion: Droplet size, zeta-potential, emulsifying properties, and rheological behavior, Food Hydrocolloid 98 (2020) 105306-.
[8] M.R. Olthof, P. Hollman, M.B. Katan, Chlorogenic acid and caffeic acid are absorbed in humans, J. Nutr. 131 (1) (2001) 66–71.
[9] N. Yun, J.W. Kang, S.M. Lee, Protective effects of chlorogenic acid against ischemia/reperfusion injury in rat liver: molecular evidence of its antioxidant and anti-inflammatory properties, J. Nutr. Biochem. 23 (10) (2012) 1249–1255.
[10] S. Ren, M. Wu, J. Guo, W. Zhang, X. Liu, L. Sun, R. Holyst, S. Hou, Y. Fang, X. Feng, Sterilization of polydimethylsiloxane surface with Chinese herb extract: a new antibiotic mechanism of chlorogenic acid, Sci. Rep.-UK 5 (2015) 10464.
[11] J. Santana-Gálvez, L. Cisneros-Zevallos, D. Jacobo-Velázquez, Chlorogenic Acid: recent advances on its dual role as a food additive and a nutraceutical against metabolic syndrome, Molecules 22 (3) (2017) 358, https://doi.org/10.3390/molecules22030358.
[12] T. Wang, X. Chen, W. Wang, L. Wang, L. Jiang, D. Yu, F. Xie, Effect of ultrasound on the properties of rice bran protein and its chlorogenic acid complex, Ultrason. Sonochem. 79 (2021) 105758, https://doi.org/10.1016/j.ultsonch.2021.105758.
[13] B.E. Elizalde, A.M.R. Pilosof, G.B. Bartholomai, Prediction of emulsion instability from emulsion composition and physicochemical properties of proteins, J. Food Sci. 56 (1) (1991) 116–120.
[14] A. Xz, A. Bq, A. Fx, H.A. Miao, A. Ys, H.A. Lu, L.A. Liang, Z.A. Shuang, L. Yang, Emulsion stability and dilatational rheological properties of soy/whey protein isolate complexes at the oil-water interface: influence of pH, Food Hydrocolloid (2020).
[15] D. Rousseau, Fat crystals and emulsion stability — a review, Food Res. Int. 33 (1) (2000) 3–14.
[16] P. Ma, Q. Zeng, K. Tai, X. He, Y. Yao, X. Hong, F. Yuan, Preparation of curcumin-loaded emulsion using high pressure homogenization: Impact of oil phase and concentration on physicochemical stability, LWT – Food Sci. Technol. 84 (2017) 34–46.
[17] L. Lee, I.T. Norton, Comparing droplet breakup for a high-pressure valve homogeniser and a Microfluidizer for the potential production of food-grade nanoemulsions, J. Food Eng. 114 (2) (2013) 158–163.
[18] N. Sharma, G. Kaur, S.K. Khatkar, Optimization of emulsification conditions for designing ultrasound assisted curcumin loaded nanoemulsion: Characterization, antioxidant assay and release kinetics, LWT – Food Sci. Technol. 141 (2021), 110962.
[19] S. Manickam, K. Sivakumar, C.H. Pang, Investigations on the generation of oil-in-water (O/W) nanoemulsions through the combination of ultrasound and microchannel, Ultrason. Sonochem. 69 (2020) 105258, https://doi.org/10.1016/j.ultsonch.2020.105258.
[20] O.A. Higuera-Barraza, C.L. Del Toro-Sanchez, S. Ruiz-Cruz, E. Márquez-Ríos, Effects of high-energy ultrasound on the functional properties of proteins, Ultrason. Sonochem. 31 (2016) 558–562.
[21] L. Zhou, J. Zhang, L. Xing, W. Zhang, Applications and effects of ultrasound assisted emulsification in the production of food emulsions: A review, Trends Food Sci. Technol. 110 (2021) 493–512.
[22] J. O'Sullivan, B. Murray, C. Flynn, I. Norton, The effect of ultrasound treatment on the structural, physical and emulsifying properties of animal and vegetable proteins, Food Hydrocolloid 53 (2016) 141–154.
[23] M. Corredig, E. Verespej, D.G. Dalgleish, Heat-induced changes in the ultrasonic properties of whey proteins, J. Agric. Food Chem. 52 (14) (2004) 4465–4471.
[24] Y. Zhu, Y. Lu, B. Gao, D. Wang, G. Yang, C. Guo, Ultrasonic-assisted emulsion synthesis of well-distributed spherical composite CL-20@PNA with enhanced high sensitivity, Mater. Lett. 205 (oct.15) (2017) 94–97.
[25] A. Cucheval, R.C.Y. Chow, A study on the emulsification of oil by power ultrasound, Ultrason. Sonochem. 15 (5) (2008) 916–920.
[26] H. Liu, J. Zhang, H. Wang, Q. Chen, B. Kong, High-intensity ultrasound improves the physical stability of myofibrillar protein emulsion at low ionic strength by destroying and suppressing myosin molecular assembly, Ultrason. Sonochem. 74 (2021) 105554, https://doi.org/10.1016/j.ultsonch.2021.105554.
[27] Y. Liang, G. Gillies, L. Matia-Merino, A. Ye, H. Patel, M. Golding, Structure and stability of sodium-caseinate-stabilized oil-in-water emulsions as influenced by heat treatment, Food Hydrocolloid 66 (2017) 307–317.
[28] Y. Xu, J. Wu, S. Wang, Comparative study of whey protein isolate and gelatin treated by pH-shifting combined with ultrasonication in loading resveratrol, Food Hydrocolloid 117 (2021) 106694, https://doi.org/10.1016/j.foodhyd.2021.106694.
[29] J. Jiang, B.o. Zhu, Y. Liu, Y.L. Xiong, Interfacial structural role of ph-shifting processed pea protein in the oxidative stability of oil/water emulsions, J. Agric. Food. Chem. 62 (7) (2014) 1683–1691.
[30] Q. Li, J. Zheng, G.e. Ge, M. Zhao, W. Sun, Impact of heating treatments on physical stability and lipid-protein co-oxidation in oil-in-water emulsion prepared with soy protein isolates, Food Hydrocolloid 100 (2020) 105167, https://doi.org/10.1016/j.foodhyd.2019.06.012.
[31] H. Li, F. Li, X. Wu, W. Wu, Effect of rice bran rancidity on the emulsion stability of rice bran protein and structural characteristics of interface protein, Food Hydrocolloids 121 (2021) 107006, https://doi.org/10.1016/j.foodhyd.2021.107006.
[32] A. Ym, A. Zl, A. Cz, B. Sh, A. Hh, D.A. Peng, A. Al, S.A. Hong, B. Cla, A. Ll, Ultrasonic modification of whey protein isolate: Implications for the structural and functional properties, LWT (2021).
[33] D. Li, X. Li, G. Wu, P. Li, H. Zhang, X. Qi, L. Wang, H. Qian, The Characterization and Stability of the Soy Protein Isolate / 1-Octacosanol Nanocomplex, Food Chem 297(NOV.1) (2019) 124766.1-124766.7.
[34] D. Wu, C. Wu, W. Ma, Z. Wang, C. Yu, M. Du, Effects of ultrasound treatment on the physicochemical and emulsifying properties of proteins from scallops Chlamys farreri, Food Hydrocolloid 89 (2019) 707–714.
[35] F. Zha, S. Dong, J. Rao, B. Chen, Pea protein isolate-gum Arabic Maillard conjugates improves physical and oxidative stability of oil-in-water emulsions, Food Chem. 285 (JUL.1) (2019) 130–138.
[36] J. Nishad, A. Dutta, S. Saha, S.G. Rudra, E. Varghese, R.R. Sharma, M. Tomar, M. Kumar, C. Kaur, Ultrasound-assisted development of stable grapefruit peel polyphenolic nano-emulsion: Optimization and application in improving oxidative stability of mustard oil - ScienceDirect, Food Chem. 334 (2021) 127561, https://doi.org/10.1016/j.foodchem.2020.127561.
[37] Y.R. Tang, S. Ghosh, Stability and rheology of canola protein isolate-stabilized concentrated oil-in-water emulsions, Food Hydrocolloid 113 (2021) 106399, https://doi.org/10.1016/j.foodhyd.2020.106399.

[38] B.J. Kemps, F.R. Bamelis, K. Mertens, E.M. Decuypere, J.G. De Baerdemaeker, B. De Ketelaere, The assessment of viscosity measurements on the albumen of consumption eggs as an indicator for freshness, Poult. Sci. 89 (12) (2010) 2699–2703.
[39] C.-H. Tang, L. Shen, Role of conformational flexibility in the emulsifying properties of bovine serum albumin, J. Agric. Food. Chem. 61 (12) (2013) 3097–3110.
[40] O. Shamsara, Z.K. Muhidinov, S.M. Jafari, J. Bobokalonov, A. Jonmurodov, M. Taghvaei, M. Kumpugdee-Vollrath, Effect of ultrasonication, pH and heating on stability of apricot gum-lactoglobuline two layer nanoemulsions, Int. J. Biol. Macromol. 81 (2015) 1019–1025.
[41] Q.A. Al-Maqtari, A. Ghaleb, A.A. Mahdi, W. Al-Ansi, W. Yao, Stabilization of water-in-oil emulsion of pulicaria jaubertii extract by ultrasonication: fabrication, characterization, and storage stability, Food Chem. 350 (2) (2021), 129249.
[42] C. Botella-Martínez, J. Fernández-López, J. Pérez-Lvarez, M. Viuda-Martos, Gelled Emulsions Based on Amaranth Flour with Hemp and Sesame Oils, (2020).
[43] N. Cumby, Y. Zhong, M. Naczk, F. Shahidi, Antioxidant activity and water-holding capacity of canola protein hydrolysates, Food Chem. 109 (1) (2008) 144–148.
[44] N.P. Boralugodage, R.J. Arachchige, A. Dutta, G.W. Buchko, W.J. Shaw, Evaluating the role of acidic, basic, and polar amino acids and dipeptides on a molecular electrocatalyst for H2 oxidation, Catal. Sci. Technol. 7 (5) (2017) 1108–1121.
[45] B. Niu, P. Shao, P. Sun, Ultrasound-assisted emulsion electrosprayed particles for the stabilization of β-carotene and its nutritional supplement potential, Food Hydrocolloid 102 (2019), 105634.
[46] M. Ai, Z. Zhang, H. Fan, Y. Cao, A. Jiang, High-intensity ultrasound together with heat treatment improves the oil-in-water emulsion stability of egg white protein peptides – ScienceDirect, Food Hydrocolloid 111 (2021) 106256, https://doi.org/10.1016/j.foodhyd.2020.106256.